PERGAMON

Vision Research 40 (240) 2329–2339

Vision Research

www.elsevier.com/locate/visres

Seeing circles: what limits shape perception?

Dennis M. Levi [a,*], Stanley A. Klein [b]

[a] *University of Houston, College of Optometry, Houston, TX 77204-6052, USA*
[b] *University of California, School of Optometry, Berkeley, CA 94720-2020, USA*

Received 14 July 1999; received in revised form 7 February 2000

Abstract

Humans are remarkably adept at judging shapes and discriminating forms. Forms and shapes are initially sampled by discrete localized visual filters (or receptive fields) in 'early' stages of visual processing. However, more complex higher level filters which integrate or pool information from many local filters may be needed to discern shapes. In order to understand the mechanisms that limit shape perception we asked observers to detect distortions in the shape of briefly presented circles constructed out of samples (Gabor patches, which are well matched to the early visual filters), and varied the radius of the circle, and the number and orientation of the samples. Our results show that shape perception is determined by two factors: the primary determinant is the separation between the samples; however, the orientation of the samples can modulate performance. At small separations, performance is best when the samples are aligned with the global shape, poorer when they are orthogonal, and intermediate when they are all horizontal or vertical. At larger separations these contextual differences disappear; however at all separations, performance is reduced when the orientations of the samples are mixed (i.e. each sample is randomly either aligned or orthogonal, or randomly either horizontal or vertical.). These results suggest an important role for sample separation in shape perception for sampled shapes and suggest that the mechanisms involved in feature binding may modulate the responses of the mechanisms underlying shape perception.

Keywords: Shape perception; Circles; Visual processing

1. Introduction

Humans are remarkably adept at judging shapes and discriminating forms. For example, we are able to judge the height-to-width ratio of squares and circles with a precision of 2–3% of the diameter of the form (Regan & Hamstra, 1992; Saarinen & Levi, 1999, 2000; Zanker & Quenzer, 1999). Recent studies suggest that we are able to discern even smaller distortions (bumps) in the shape of a circle (Wilkinson, Wilson & Habak, 1998). While it is widely believed that forms and shapes are initially sampled by discrete localized visual filters (or receptive fields) in 'early' stages of visual processing, more complex higher level filters which integrate or pool information from many local filters may be needed to discern shapes (Wilkinson et al., 1998). Indeed, Wilkinson et al. argue that their very low Weber fractions for seeing distortions in circles must result from global processing at higher levels. Wilkinson et al. specified their performance as a fraction of the circle radius. However, it is not clear that the radius per se plays a critical or general role in limiting shape perception, since other aspects of the stimulus may have co-varied with the circle radius. Thus, one goal of the present study was to clarify the role of circle radius in shape perception.

Recent physiological (Kapadia, Ito, Gilbert & Westheimer, 1995; Gilbert, Das, Ito, Kapadia & Westheimer, 1996; Lamme & Spekreijse, 1998; Polat, Mizobe, Pettet, Kasamatsu & Norcia, 1998) work suggests that elements with orientations that match the contour may 'bind' (i.e. be linked) to produce a coherent percept of shape. Binding of the features that define a form is particularly important when the form is surrounded by other nearby features, which might camouflage the form; however, binding of features is also critical for seeing coherent shapes.

Psychophysical work also suggests that orientations that match the contour may enhance contour detection

* Corresponding author. Fax: +1-713-7431888.
E-mail address: dlevi@uh.edu (D.M. Levi).

0042-6989/00/$ - see front matter
PII: S0042-6989(00)00092-4

either at detection threshold (Polat & Sagi, 1993; Kapadia et al., 1995; Saarinen, Levi & Shen, 1997; Bonneh & Sagi, 1998; Levi & Sharma, 1998), or when the target 'contour' is embedded in distractors (Hayes & Hess, 1993; Kovacs & Julesz, 1993; Pettet, McKee & Grzywacz, 1998). However, to date there has been conflicting evidence for similar context effects in position or shape judgements. For example, alignment thresholds for Gabor patches are reported to be similar when the local features (i.e. the carrier grating) are aligned with the global configuration (i.e. the overall orientation of the three patches) and when they are orthogonal (Kooi, De Valois & Switkes, 1991; Keeble & Hess, 1998). Detecting position jitter in a path is also not influenced by whether the local feature orientations are aligned with or orthogonal to the path (Keeble & Hess, 1999). On the other hand, the aspect ratio of a square can be judged more precisely when the local features are aligned with the global contour than when they are orthogonal to it (Saarinen & Levi, 1999). Similarly, the orientation of a C-like figure can be discerned at a lower contrast when the local features are aligned with the C-contour than when they are orthogonal to it (Saarinen & Levi, 2000). Thus, context (feature orientation) seems to matter for certain tasks and stimuli but not for others.

Why does context matter for certain tasks and stimuli and not others? One critical aspect of context effects (and for most of the models proposed to explain them) is that context effects occur over limited distances (e.g. Field, Hayes & Hess, 1993; Polat & Sagi, 1993; Bonneh & Sagi, 1998). Many simple position tasks also show significant 'context' effects at small distances but not at large distances. For example, at small separations width discrimination (Levi & Westheimer, 1987), bisection (Levi, Jiang & Klein, 1990) and Vernier alignment (O'Shea & Mitchell, 1990; Levi & Waugh, 1996; Beard, Levi & Klein, 1997) are more precise when the features have the same stimulus polarity. However, at large separations thresholds are essentially identical for same- and mixed-polarity features. Thus the separation of the features may be a critical determinant of whether context effects occur or not. In their alignment experiment, Kooi et al. (1991) reported no difference in alignment thresholds for Gabor patches that both had vertical carriers (and were thus coaxial), horizontal carriers (and were thus ortho-axial), or were mixed. In their study the patches were separated by 25 min or 2.5 times the spatial period of the 6 c/deg grating. Similarly, Keeble and Hess (1998) used patches separated by 160 min or six times the carrier period.

Although humans can localize the envelope of a Gabor patch precisely when the interpatch separation is large (Toet & Koenderink, 1988), observers are likely to use the carrier information for spatial localization when the separation is small (about 2 wavelengths or less) and to use the envelope to localize when the separation is larger (Akutsu, McGraw & Levi, 1999). In line with this idea, it is noteworthy that in their study with circles, Keeble and Hess (1999) found little influence of orientation for their 'standard' condition (separation 40′ or three times the spatial period of the 4.5 c/deg carrier grating); however, at the smallest separation (20′) both observers show a highly significant effect of orientation, with thresholds at least a factor of two better for tangential gratings (i.e. aligned with the circle) than for radial gratings (orthogonal to the circle).[1] Keeble and Hess (1999) varied the separation by varying the number of patches and their results suggest that number or separation plays an important role in shape perception.

The purpose of the present study was to try to clarify the role of circle radius, sample separation and orientation in shape perception. In order to understand the mechanisms that limit shape perception we asked observers to detect distortions in the shape of briefly presented circles constructed out of samples (Gabor patches, which are well matched to the early visual filters), and varied the radius of the circle, and the number and orientation of the samples. We chose circles because curvature (Attneave, 1954) and contour closure (Kovacs & Julesz, 1993) are considered to be crucially important in object recognition. Our results show that shape perception is not determined by the circle radius. Rather, it is limited primarily by two factors: the separation between the samples, and their orientation. These factors have little (separation) or no (orientation) effect on contrast discrimination for similar stimuli. These results provide strong constraints on the mechanisms for shape perception.

2. Methods

2.1. Stimuli

The circle shape, defined by N samples (usually Gabor patches, but in some experiments Gaussian patches), was displayed on a Monoray high brightness monitor using a Cambridge Research Systems VSG 213 graphics card with 15 bit contrast resolution. The Gabor patches were constructed by multiplying a sinusoid by a Gaussian (in cosine phase). These patches had a bandwidth of ≈ 1.1 octaves (0.5 cycles/SD), a peak contrast of 100%, and a mean luminance of approximately 80 cd/m^2.

[1] It is worth noting that in all of the cited studies, the envelope standard deviation was small relative to the separation. In previous studies with both Gaussian and Gabor stimuli we found that when the standard deviation was greater than about one-third of the separation, thresholds were constrained by the standard deviation of the Gaussian envelope (e.g. Levi, Jiang & Klein, 1990).

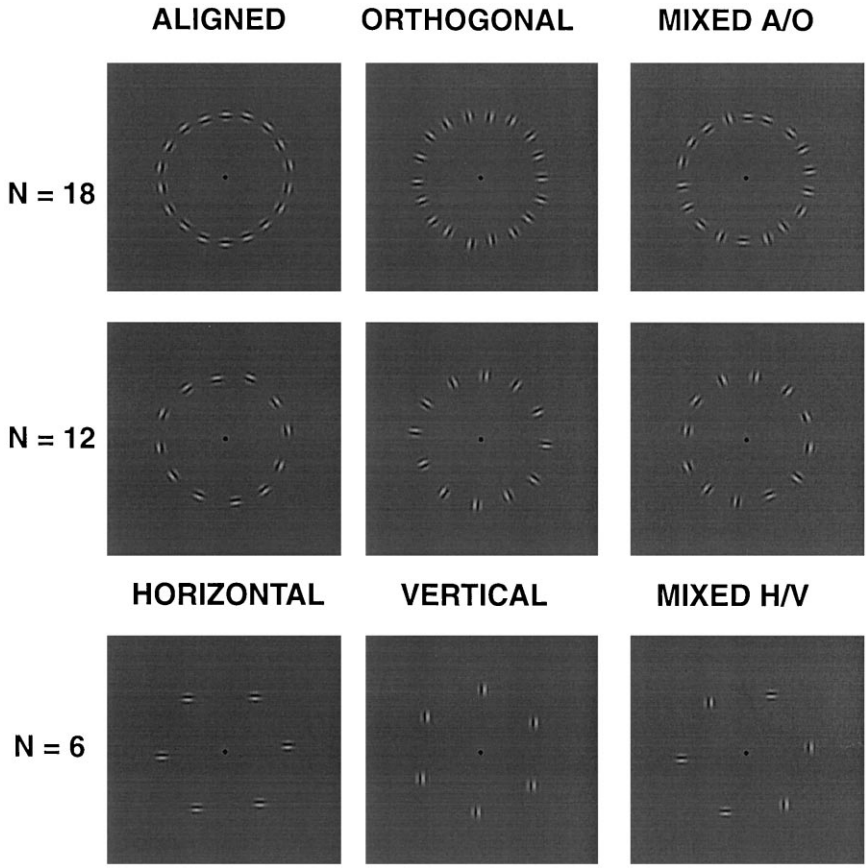

Fig. 1. Examples of the stimuli used in our experiments. Each row shows circles constructed from samples (Gabor patches) which vary in number, N, from $N = 18$ (top) to $N = 6$ (bottom). The columns represent different sample orientations (for the top two rows, aligned (left), orthogonal (center) and mixed aligned/orthogonal (right). For the bottom row, horizontal (left), vertical (center) and mixed horizontal/vertical (right)). Note that in each panel the perturbation is the same magnitude (approximately 2% of the circle radius); however, it is seen most easily with $N = 18$ and with the orientations aligned.

The observer viewed the screen monocularly, with normal overhead illumination, and fixated a black square (0.05°), which was constantly present at the center of the screen. We took two precautions to ensure that the fixation target did not provide a useful cue for shape discrimination. First, while the angular separation of the samples around the notional circle was determined by N, the actual positions of all of the samples varied randomly (by varying the position on the circle of the 'first' sample). Second, the location of the entire circle was randomly offset from the center, by a uniform jitter (approximately twice the threshold) independently in one of eight orientations (at 45° intervals). Examples of the stimuli with different N (rows) and orientations (columns) are shown in Fig. 1.

2.2. Psychophysical methods

2.2.1. Shape discrimination

To measure the precision of shape perception we presented the circle briefly (0.2 s), and on each trial, the sample positions were perturbed by one of five magnitudes of two-dimensional Gaussian jitter (applied independently to the x and y directions, and specified by the standard deviation (SD)) presented at random: 0, 1, 2, 3 or 4 times the step. The step size was determined in preliminary experiments for each observer and stimulus condition so that the threshold fell within the range of stimulus values. Following each trial the observer rated the magnitude of the perturbation (from 0 to 4), and was given auditory feedback corresponding to the actual magnitude (i.e. the SD of the jitter on that trial). A criterion-free estimate of the precision of shape perception was obtained from the rating scale data using a signal-detection method to estimate the perturbation threshold (i.e. the magnitude of Gaussian jitter that could be detected on 84% of the trials, i.e. at $d' = 1$) (Levi & Klein, 1990). The thresholds reported here represent the average of at least four blocks of 125 trials/block, weighted by the inverse variance. The error bars shown in the figures represent ± 1 SEM, and include both within and between run variation.

From run to run we either fixed the circle radius and varied N, or fixed N and varied the radius. Radius was

varied by changing the observer's viewing distance. This method has the advantage of maintaining stimulus visibility at a nearly constant level (as indicated by the nearly constant contrast JND) by increasing the Gaussian SD and lowering the spatial frequency (SF) with increasing eccentricity (shorter viewing distance). The 10-fold range of viewing distances (from 4 to 0.4 m), resulted in SD varying from 1.6′ to 16′, and SF varying from $\approx$19 to 1.9 c/deg. In the fixed N experiments, the separation was always five times the grating period or ten times the SD. Control experiments (not shown), in which viewing distance and sample dimensions are fixed and radius varied (over a range where the patches are visible), give essentially identical results.

2.2.2. Contrast discrimination

To measure the precision of contrast perception we presented the circle briefly (0.2 s), and on each trial, the samples were presented at one of five suprathreshold contrast levels: at the 'base' contrast (60%) or one or two steps higher or lower than the base contrast. The step size was determined in preliminary experiments for each observer and stimulus condition so that the threshold fell within the range of stimulus values. Following each trial the observer rated the magnitude of the contrast (from -2 to 2), and was given auditory feedback corresponding to the actual magnitude. A criterion-free estimate of the precision of contrast discrimination was obtained from the rating scale data using a signaldetection method to estimate the contrast discrimination threshold (also specified at $d' = 1$). The thresholds reported here represent the average of at least four blocks of 125 trials/block, weighted by the inverse error. The error bars shown in the figures represent ± 1 SEM, and include both within and between run variation.

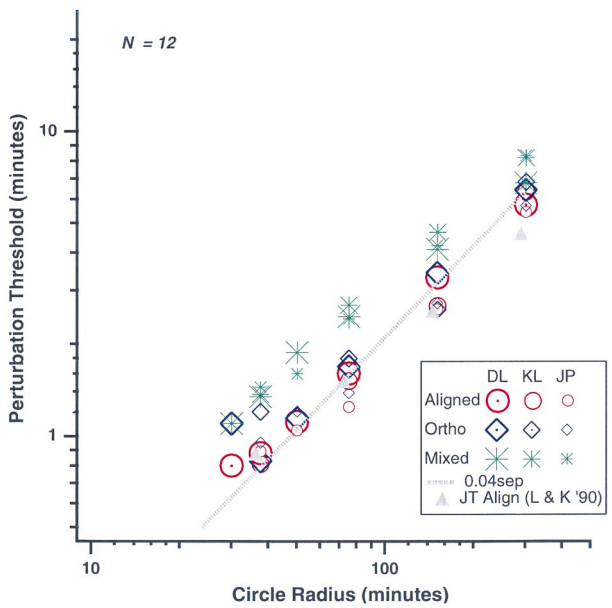

Fig. 2. The effect of circle radius. Perturbation thresholds (in arcmin) are plotted as a function of circle radius for a circle consisting of 12 equally spaced samples. The sample's carrier was oriented aligned with the circle contour, orthogonal to it or mixed. Data are shown for three observers. The line shows threshold equal to 4% of the separation between samples (for separations corresponding to $N = 12$ at any given radius). The gray triangles are JT's 3-line Vernier alignment thresholds on an iso-eccentric arc from Fig. 6 of Levi and Klein (1990). See text for details.

3. Results

3.1. The role of radius

Consistent with previous reports (Wilkinson et al., 1998), the perturbation threshold is proportional to the circle radius (Fig. 2). When the orientation of the 12 samples comprising the circle was either aligned with, or orthogonal to the circle, perturbation thresholds were about 2% of the circle radius. Interestingly, performance was consistently poorer (thresholds were higher), when the sample orientations were mixed (i.e. each sample was randomly either aligned or orthogonal to the circle contour). The effect of orientation will be examined and quantified in detail in Section 3.3.

3.2. The role of N (the number of samples)

Varying the radius of our sampled circle alters both the eccentricity of the samples and the inter-sample separation. There is considerable evidence that both eccentricity and separation dependent processes can limit spatial judgements (Sullivan, Oatley & Sutherland, 1972; Beck & Halloran, 1985; Klein & Levi, 1987; Morgan & Watt, 1989; Levi & Klein, 1990; Whitaker & Latham, 1997). In order to assess the relative importance of eccentricity and separation in determining performance, we fixed the circle radius (and therefore the eccentricity of the samples) and varied the number, N, of uniformly spaced samples around the circle. Varying N only alters the separation between the samples. Consistent with Keeble and Hess (1999) we found that the precision of shape perception depends strongly on the number of samples (Fig. 3). Note that in this experiment, the circle radius is constant. When the sample orientations are consistent (i.e. all aligned, all orthogonal, all horizontal or all vertical), the perturbation threshold is approximately inversely proportional to N.

There are several rather surprising aspects of these results which suggest that N is not the fundamental limiting factor in shape perception. First, for similar orientations, the precision of shape perception is directly proportional to N, and inversely proportional to radius. This finding implies that radius and N can be

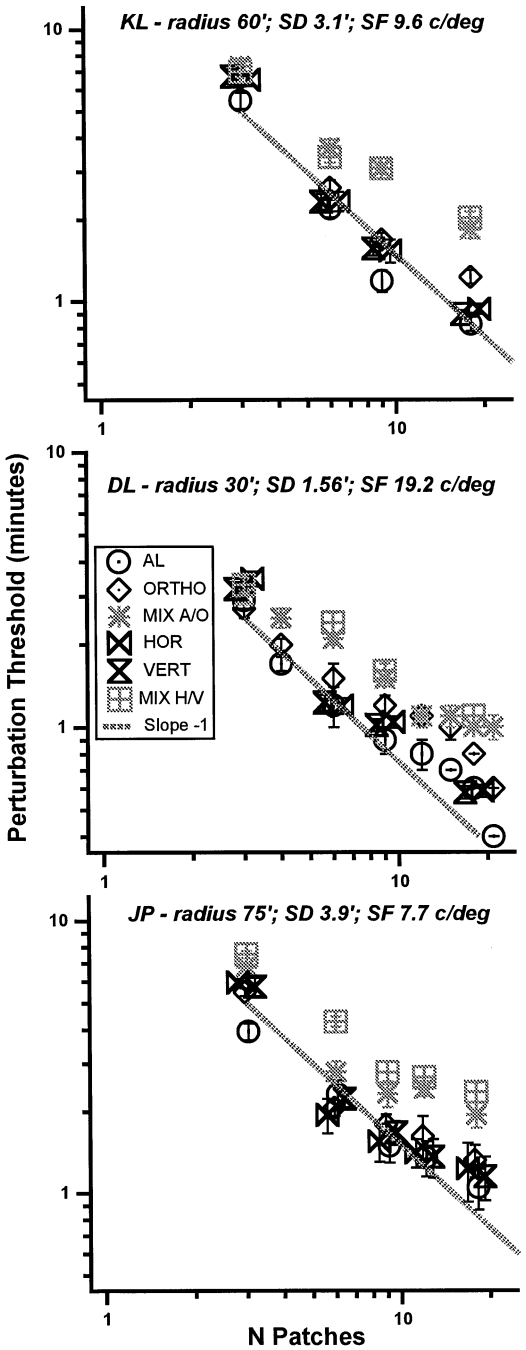

Fig. 3. The effect of the number of samples (N). Perturbation thresholds (in arcmin) are plotted as a function of N for circles of fixed radii. The radii were different for each observer. The sample's carrier was oriented aligned with the circle contour, orthogonal to it, mixed aligned/orthogonal, horizontal, vertical or mixed horizontal/vertical. Data are shown for three observers. The lines (slope $= -1$) show threshold inversely proportional to N.

traded off with no loss of precision, and indeed, we find that thresholds are similar with a radius of approximately 16 min and $N = 6$, and with larger radii and proportionally larger N. Varying either the radius or the number of samples (in a circle of fixed radius) alters the separation between the samples. The critical point (Fig. 4) is that when the separation between patches is held constant (at 16′), thresholds are essentially identical regardless of radius or N (Beck & Halloran, 1985). The importance of separation has been known for over a century (Fechner, 1858), and is often referred to as 'Weber's Law' for position (Morgan & Watt, 1989; Levi & Klein, 1990). Second, an ideal observer model (i.e. a machine which knows the stimulus exactly, and uses each sample to provide an independent estimate of the shape) predicts that performance on our task should improve in proportion to the square root of N, rather than in direct proportion to N (Levi & Klein, 1986) which is what we found. Thus, as suggested by Keeble and Hess (1999) it is the separation between samples rather than the number of samples that limits performance.

3.3. The role of orientation

To examine the role of separation and orientation in judging shape, we have replotted the results of Figs. 2 and 3 with the abscissa specified as the inter-sample separation, and the threshold specified as a 'Weber fraction', i.e. threshold/separation (Fig. 5). When plotted in this way, the fixed N data (Fig. 5 top) are an approximately constant Weber fraction (roughly 4% of the separation) for similarly oriented samples. Thus, under these conditions performance is 'scale invariant', i.e. we can judge the shape of a circle (of fixed physical size) with equal precision at any viewing distance. Interestingly, detection of curvature in lines is also scale invariant (Whitaker & McGraw, 1998). For comparison, thresholds are also shown for detecting perturbations in the positions of a straight horizontal string of

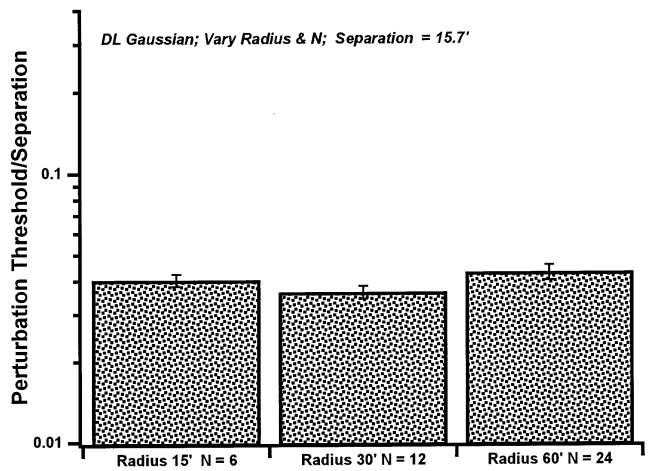

Fig. 4. Circle radius and number of samples can trade-off. Perturbation thresholds for observer DL (specified as a fraction of the inter-sample separation) are shown for circles with radii of 15′, 30′ and 60′ and $N = 6$, 12 and 24, respectively. The samples were Gaussians. For each of these conditions, the inter-sample separation is the same (15.7′) and the thresholds are essentially identical.

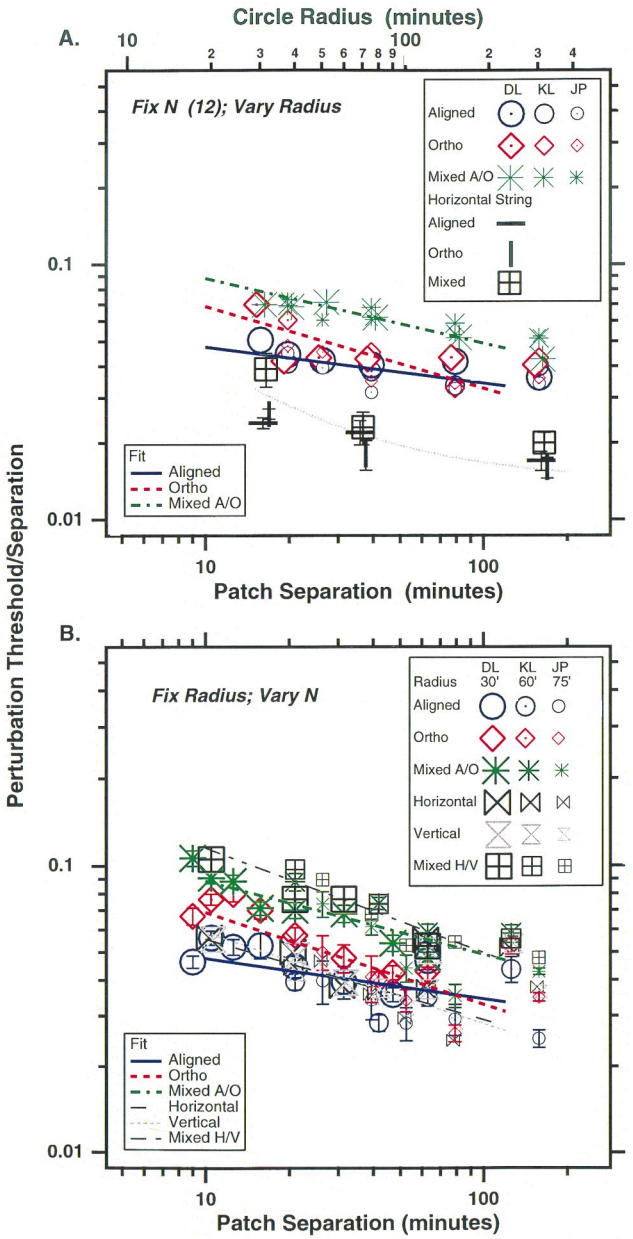

Fig. 5. Top: Perturbation thresholds from Fig. 3 (vary radius) are replotted, specified as a Weber fraction of the inter-sample separation versus separation. The lines are the model fit to the group data (described in the Appendix). For comparison thresholds are shown for detecting disorder in a horizontal string of seven patches (similar to those used for Fig. 3 The dotted line fit to the string data is an 'eccentricity' fit (Levi & Klein, 2000). Bottom: Perturbation thresholds from Fig. 2 (vary N) are replotted, specified as a Weber fraction of the inter-sample separation versus separation.

five separated patches (similar in their details to those used in Figs. 1–3 for circularly arranged samples). It is of some interest to note that the Weber fractions for the string of separated patches are always lower than for the circle. Observers are more acute at judging deviations from a line than from a circle. Unlike the circle, the Weber fractions for the string of well-separated patches are not strongly dependent on the similarity in orientation of the samples. Interestingly, the string data are reasonably well predicted by an eccentricity dependent mechanism (described in Levi & Klein, 2000 — shown by the dotted line in Fig. 5).

When the circle radius is fixed and the number of samples varied (Fig. 5 bottom), the Weber fraction increases modestly as the separation decreases (as it does in Fig. 5 top). This variation in the Weber fraction for circular shapes is consistent with the variation in the Weber fraction for other tasks involving position judgements (Levi & Klein, 1987, 1990; Whitaker & Latham, 1997), and is also evident for the string. We suspect that when stimulus samples of a fixed size are packed closely relative to the visual nervous systems' sampling, the sample positions cannot be as precisely localized. However, it is clear that the separation of the samples is a critical factor in limiting shape perception, and that the sample orientation can modulate performance.

The precision of shape perception depends mainly on sample separation, but it is also modulated by orientation. The Appendix describes two separate analyses used to assess the role of separation and orientation. At small sample separations (e.g. 10′ Fig. 5, and Tables 1 and 2) performance is best (Weber fractions lowest) when the samples are aligned, worst when they are mixed and about midway between when they are orthogonal. The height/width ratio of squares is also judged more acutely when the local orientations of samples along the edges are aligned with the shape than when they are orthogonal (Saarinan & Levi, 1999). Interestingly, Weber fractions with vertical and horizontal closely spaced samples (which are not aligned with the contour) fall between those for aligned and orthogonal samples, and mixed horizontal/vertical are worst of all (a factor of 2.3 ± 0.2 worse than the aligned case). While these orientation effects are highly significant at small separations ($P < 0.001$) they diminish at large separations (e.g. 120′ — Fig. 5, and Tables 1 and 2). However, shape discrimination remains significantly poorer for the mixed conditions ($P < 0.001$). Keeble and Hess (1999) also noted that randomizing the sample orientation degraded performance. These context effects in shape perception are interesting and may be important in understanding the underlying neural mechanisms involved in shape perception.

Interestingly, while separation and orientation play a critical role in shape discrimination and contrast detection (Polat & Sagi, 1993; Bonneh & Sagi, 1998) they have a rather different effect on contrast discrimination (Fig. 6). Shape thresholds are proportional to separation (and inversely proportional to N), while contrast discrimination thresholds increase only slightly with increasing separation (mean slope ≈ 0.25). We varied separation by changing N^2, so the 1/4 root variation in

[2] For DL, $N = 3$, 12 and 24 and for KL, $N = 3$, 12 and 18.

contrast discrimination thresholds with separation that is evident here is consistent with the $-1/4$ root (slope -0.25) improvement of contrast detection thresholds with increasing N reported by Bonneh and Sagi (1998). Interestingly, there is no effect of orientation on contrast discrimination at any separation. While shape discrimination is enhanced for closely spaced aligned samples (relative to orthogonal) and degraded for mixed samples, contrast discrimination shows no orientation effect.

4. Discussion

Shape perception is very acute when the samples are similar. Previous studies (e.g. Wilkinson et al., 1998)

Table 1
Parameters of the model fit to Fig. 5 (see Appendix A)

Orientation	Obs	% Weber (10′)		% Weber (120′)		Slope
		Fit 1	Fit 2	Fit 1	Fit 2	
Aligned						
	KL	4.28 ± 0.16	4.60	3.35 ± 0.22	3.53	
	DL	4.96 ± 0.12	4.87	3.88 ± 0.17	3.74	
	JP	4.09 ± 0.16	4.07	3.20 ± 0.22	3.12	
	Group	4.77 ± 0.12		3.35 ± 0.21		-0.14 ± 0.03 (-0.11)
Orthogonal						
	KL	6.70 ± 0.24	6.57	3.42 ± 0.55	3.33	
	DL	6.94 ± 0.17	6.96	3.55 ± 0.4	03.52	
	JP	5.54 ± 0.23	5.82	2.83 ± 0.54	2.94	
	Group	6.87 ± 0.17		3.10 ± 0.43		-0.32 ± 0.04 (-0.27)
Mixed A/O						
	KL	8.54 ± 0.28	8.47	4.98 ± 0.47	4.94	
	DL	8.92 ± 0.22	8.97	5.20 ± 0.36	5.23	
	JP	7.17 ± 0.40	7.50	4.18 ± 0.6	84.38	
	Group	8.85 ± 0.20		4.69 ± 0.36		-0.26 ± 0.03 (-0.22)
Horizontal						
	KL	5.07 ± 0.28	5.47	3.12 ± 0.25	2.91	
	DL	5.51 ± 0.23	5.79	3.30 ± 0.21	3.09	
	JP	4.46 ± 0.44	4.84	2.75 ± 0.40	2.58	
	Group	5.56 ± 0.21		2.76 ± 0.25		-0.28 ± 0.04 (-0.25)
Vertical						
	KL	5.53 ± 0.35	5.18	2.95 ± 0.38	3.08	
	DL	5.76 ± 0.25	5.49	3.08 ± 0.27	3.27	
	JP	4.74 ± 0.55	4.59	2.53 ± 0.59	2.73	
	Group	5.87 ± 0.24		2.66 ± 0.28		-0.32 ± 0.05 (-0.21)
Mixed H/V						
	KL	13.25 ± 0.90	10.6	24.43 ± 1.32	5.20	
	DL	11.19 ± 0.59	11.25	3.74 ± 0.86	5.51	
	JP	13.20 ± 1.12	9.40	4.41 ± 1.63	4.60	
	Group	11.51 ± 0.56		4.67 ± 0.90		-0.36 ± 0.05 (-0.29)

Table 2
Weber fractions relative to orthogonal orientation (see Appendix A)

	Sep 10′		Sep 120′	
Condition	Weber fraction	P (2 tailed)	Weber fraction	P (2 tailed)
1-Normalized orthogonal	1		1	
2-Aligned factor	0.70 ± 0.04	$<10^{-6}$	1.06 ± 0.06	0.4
3-Mixed A/O factor	1.29 ± 0.07	0.0003	1.49 ± 0.10	0.00001
4-Horizontal	0.83 ± 0.07	0.02	0.88 ± 0.12	0.3
5-Vertical factor	0.79 ± 0.04	0.001	0.93 ± 0.10	0.5
6-Mixed H/V factor	1.62 ± 0.09	0.0001	1.56 ± 0.14	0.0001

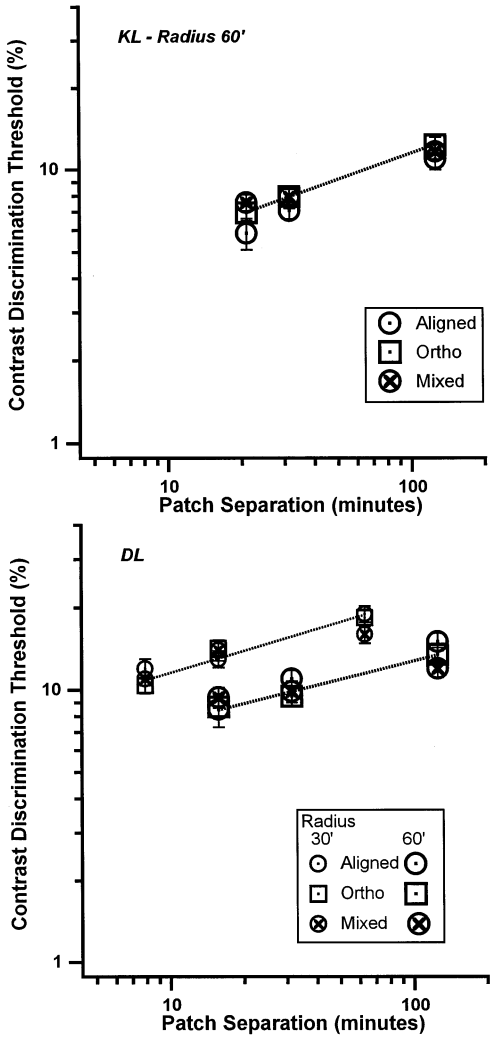

Fig. 6. Contrast discrimination thresholds versus separation for two observers. Separation was varied by changing N. Contrast discrimination thresholds increase only slightly with increasing separation. The lines show power functions fit to the data. The mean exponent (slope on log–log coordinates) is ≈ 0.25. Interestingly, there is *no* effect of orientation on contrast discrimination at any separation.

have linked detection of distortions in circles to curvature detection based on the assumption that circle radius is critical (since curvature is inversely proportional to radius). However, since radius and N can trade off, its is clear that the primary limiting factor is the separation between samples not the radius. Keeble and Hess (1999) arrived at a similar conclusion. Inspection of Fig. 1 enables the reader to determine this for him/herself. In this figure, each panel shows the same amount of distortion (approximately 2% of the radius), however, the perturbations are most visible when the number of samples is large (18) and aligned with the circle.

How does the visual nervous system implement this high level of precision in shape perception? While lines, edges and bars are considered to be ideal stimuli for early levels of visual processing (e.g. V1), smoothly curved shapes, like circles, are likely to be processed at higher cortical levels. For example, many neurons in inferior temporal cortex are selective for stimuli of specific boundary curvature (Schwartz, Desimone, Albright & Gross, 1983). Recently, Gallant, Braun and Van Essen (1993) have reported that some neurons in area V4 respond best to concentric circles, spirals and hyperbolic gratings.

It is not yet clear how shape is analyzed by high level visual neurons, but two general ideas have emerged. Schwartz et al. (1983) argued that shape is represented by a method known as Fourier descriptors where the radial distance of a feature as a function of angle is specified by a Fourier series. Wilkinson et al. (1998) argued for a somewhat similar global computation in which contour information is pooled relative to the center of an object. These models relate to continuous, rather than sampled circles. Our sampled stimuli and data can be related to the continuous case by considering our samples as being at the extrema of an oscillating sinusoid. For example, a Fourier shape descriptor with three cycles going around the circle, would be expected to have thresholds similar to our sampling case with $N = 6$, where the samples are placed at the peaks and troughs of the grating. Our results are not consistent with a simple pooling operation, since we can trade off the amount of contour information (N) with radius. Rather, the strong dependence on sample separation (see also Keeble & Hess, 1999), suggests that performance in our task may be limited by low level inputs to the higher level mechanisms involved in global shape analysis.

Our results are also consistent with previous evidence for a separation dependent mechanism in limiting position judgements on an arc (Morgan & Watt, 1989; Levi & Klein, 1990; Whitaker & Latham, 1997). For example, for separations smaller than the arc radius, Weber fractions for judging the separation of two patches on an arc are between 3 and 10%, consistent with the Weber fractions found in the present study (Whitaker & Latham, 1997). The close similarity between our circle judgements and the separation dependent mechanism for position, can be seen by the dotted line and gray triangles in Fig. 2. The dotted line shows threshold equal to 4% of the separation between samples (for separations corresponding to $N = 12$ at any given radius). The gray triangles in Fig. 2 are JT's 3-line Vernier alignment thresholds on an iso-eccentric arc from Fig. 6 of Levi and Klein (1990). The data were interpolated to the separations corresponding to $N = 12$ at each radius, multiplied by 1.48 to convert to $d' = 1$ (since Levi & Klein reported their thresholds at $d' = 0.675$), and multiplied by 1.73 to make the deterministic offsets of the Vernier task comparable to the 2-dimensional Gaussian jitter of the present study (see-

Appendix of Levi & Klein, 2000 for details). Both the line and the Vernier thresholds are remarkably close to our thresholds for judging distortions in the shape of a circle. Thus, we suspect that the same mechanisms that limit peripheral position judgements set important limits on judging the shape of a circle.

The significant modulatory effects of orientation may be useful in assessing likely mechanisms. For example, one possible mechanism for judging shape is to use the position labels ('local signs') associated with the underlying receptive fields to tag the sample positions, and to compare these tags to the observers' internal representation of a circle. However, a simple local sign model would not be expected to show context or orientation effects, since the position labels should be independent of sample orientation. Note that even at large separations performance for randomly mixed orientations is worse than with similar orientations, so random mixing must degrade the mechanisms involved in judging shape (see also Keeble & Hess, 1999).

The orientation effects seen in our results are consistent with recent evidence for context effects in detection (Kovacs & Julesz, 1993; Polat & Sagi, 1993; Kapadia et al., 1995; Saarinen et al., 1997; Bonneh & Sagi, 1998; Levi & Sharma, 1998; Pettet et al., 1998), and in detecting curved contours that are defined by variations in orientation, and are camouflaged by similar elements with random orientations (Nothdurft, 1987; Beck, Rosenfeld & Ivry, 1989; Field et al., 1993; Pettet et al., 1998). Curved contours ('snakes') 'pop out' from the random background when the local elements (the orientation of the Gabor patches) are aligned with the path, and this pop out is reduced when the local orientations are misaligned or orthogonal. Field et al. (1993), have argued for an 'association field' which integrates information across neighboring filters tuned to similar orientations. In their model, the strength of the linkage is constrained by both the separation and the orientation of the features. Our task does not involve figure-ground segregation, but rather shape (or curvature) extraction, and there are now several models for extracting shape or curvature which link orientation selective mechanisms (e.g. Parent & Zucker, 1989; Ullman, 1990).

Are the same mechanisms that are used for linking common curvature in the 'snake detection' task used for extracting shape in our task? Keeble and Hess (1999) argue that they are not. Their argument is predicated on their conclusion that "alignment of the carrier bars does not improve shape discrimination"; however, both our data and theirs show that alignment improves performance slightly (but significantly) at small separations (where physiological linking would be strongest). Keeble and Hess used a 'bullseye' stimulus (circularly symmetric patterns with a radial function which is a Gaussian multiplied by a sinusoid) as a clever control for the effects of orientation in their circle experiment. This stimulus, like the Gabor patches are band-limited. Interestingly, for both observers, the bullseye was best at the largest separation (80′) but fell roughly midway between tangential (aligned) and radial (orthogonal) at the smallest separation. We are in full agreement with Keeble and Hess that separation is the main determinant of shape discrimination for sampled circles; however, orientation significantly modulates that performance.

If the separation is small so that the stimuli overlap (or nearly overlap), alignment of the local features with the contour enhances performance by about 30% (Table 2), similar to the enhancement of detection thresholds seen with aligned flankers (Polat & Sagi, 1993), perhaps because of enhanced visibility at small separations. Similar enhancement is evident in the shape (aspect ratio) discrimination using 'rectangles' comprised of four closely spaced elongated Gabor patches (Saarinen & Levi, 1999). Interestingly, there appears to be no modulation of suprathreshold contrast discrimination thresholds, both in the present experiments and in those of Saarinen and Levi (1999) — in line with recent work showing that patches that are 'linked' on a path (a snake) do not appear to be of higher contrast than patches that are not 'linked' (Hess, Dakin & Field, 1998). Positional tasks such as our shape task, or Vernier alignment require a relative judgement so separation would be expected to play a critical role. On the otherhand, contrast discrimination does not involve separation as critically. For example, Hu, Klein and Carney (1993) compared Vernier and contrast discrimination for different gap sizes and found that gaps had a much more marked effect on Vernier than on contrast discrimination.

At large separations, there is little significant advantage due to alignment (Keeble & Hess, 1999); however, at all separations (even at large ones), randomly mixing orientations degrades the judgement, increasing thresholds by ≈ 30–60% (Table 2). Keeble and Hess (1999) noted that introducing random variability in other dimensions (viz. patch size and spatial frequency) also degraded performance. Interestingly, randomization of orientation does not interfere with contrast discrimination.

Why does randomization interfere with shape discrimination? Consider the mixed conditions in Fig. 1 (see also Keeble & Hess, 1999 — Fig. 3c). If one tracks the central bar, the object no longer appears like a circle. Rather, it appears to be a very wiggly object. So there must be competing cues for shape. There is the 'snake' cue that tracks local orientation, competing with the local sign cue that tracks the centroid of the samples. When the orientations are radial there are no snakes to interfere. Interestingly, for strings, randomization only interferes at the smallest separation (Fig. 5a), perhaps because for horizontal strings the task is

easier since one does not need to compute an unknown radius (cf. Levi & Klein, 1989).

In summary, shape perception is determined by two factors: the primary determinant is the separation between the samples; however, the orientation of the samples can modulate performance. At small separations, performance is best when the samples are aligned with the global shape, poorer when they are orthogonal, and intermediate when they are all horizontal or vertical. At larger separations these contextual differences disappear; however at all separations, performance is reduced when the orientations of the samples are mixed (i.e. each sample is randomly either aligned or orthogonal, or randomly either horizontal or vertical). These results suggest an important role for Weber's law in shape perception for sampled shapes and suggest that mechanisms involved in feature binding may modulate the responses of the mechanisms underlying shape perception. Finally we note the clear distinction between our task and the snake detection task. In detecting a path in which the samples are embedded in distracters, detecting a snake involves a correspondence problem where one must find matching features. Altering the orientation of the samples interferes with the correspondence (since altering the orientation makes the samples indistinguishable from the distracters).

Acknowledgements

Supported by grants ROIEY01728 and ROIEY04776 and a Core grant (P30EY07551) from the National Eye Institute, National Institutes of Health, Bethesda MD. We are grateful to Hope Marcotte–Queener for programming and to Paul McGraw for helpful comments.

Appendix A

In order to assess the role of separation and condition (orientation) we undertook two separate analyses.

A.1. Fit 1

Each of the six conditions (aligned (A), orthogonal (O) and their mixture (AO); and horizontal (H), vertical (V) and their mixture(HV)) were fit separately. Each condition was fit with four parameters: three parameters specified the separation Weber fraction for each observer at a 10 min separation. The fourth parameter was the exponent (the log–log slope) that characterizes the dependence on separation.

$$\text{Weber(separation)} = S(\text{subj})\ (\text{separation}/10)^{\text{slope}} \quad (1)$$

Thus for the full dataset there were a total of 24 parameters for the six conditions. The values in Table 1 that do not have standard errors were obtained with Fit 1.

A.2. Fit 2

All six conditions were run together (A, O, AO, H, V and HV). The *relative* sensitivity of the three observers was assumed to be fixed across the six conditions so that there would be just 14 parameters characterizing the data: six parameters for the Weber fraction of one observer for the six conditions at a 10 min separation, six more parameters for each condition's log–log slope (or equivalently, the Weber fractions at 120 min) and two parameters for the relative sensitivity of the two other observers.

The predicted Weber fraction for the first subject (KL) is given by the following equation:

$$\text{Weber}(c,\ \text{separation}) = \text{W10}(c)^{*}(\text{separation}/10)^{\text{slope}(c)} \quad (2)$$

where W10(c) and slope(c) specify the Weber fractions and slopes for the six conditions (c). The predicted Weber fraction for subject DL is a constant (one of the free parameters) times KL's thresholds and similarly for the third subject. The slope in Table 1 that is surrounded by parentheses is the slope obtained with Fit 2. The six slope parameters can be replaced by the six Weber thresholds at 10 and 120 min:

$$\text{slope} = \log(\text{W120}/\text{W10})/\log(120/10) \quad (3)$$

When doing the nonlinear regression to fit the data, the 12 parameters are chosen in a way to facilitate doing a t-test. One parameter is used for W10 for the orthogonal condition and five parameters are used for the ratio of the other condition to the orthogonal condition. Six more parameters are used in a similar fashion (one parameter for the orthogonal case and five ratios) for the 120 min separation. Table 2 shows the t-test for the hypothesis that the ratios are unity. For example, the ratio of aligned to orthogonal for the 10′ separation is $4.60/6.57 = 0.70$). The t value of $(1-0.70)/0.04 = 7.5$ corresponds to a 2-tailed P value of $< 10^{-6}$. This type of parameterization makes it easy to do a t-test to determine whether the six conditions are significantly different from each other at small (10 min) or large (120 min) separations. Two additional parameters provide a multiplicative factor that specifies how observers DL and JP deviate from observer KL. Observers DL and JP have thresholds 1.06 ± 0.03 and 0.89 ± 0.03 times observer KL's thresholds.

References

Akutsu, H., McGraw, P. V., & Levi, D. M. (1999). Alignment of well-separated patches: multiple location tags. *Vision Research*, *39*, 789–801.

Attneave, F. (1954). Some informational aspects of visual perception. *Pyschology Review*, *61*, 183–193.

Beard, B. L., Levi, D. M., & Klein, S. A. (1997). Vernier acuity with non-simultaneous targets: the cortical magnification factor estimated by psychophysics. *Vision Research*, *37*, 325–346.

Beck, J., & Halloran, T. (1985). Effects of spatial separation and retinal eccentricity on two-dot vernier acuity. *Vision Research*, *25*, 1105–1111.

Beck, L., Rosenfeld, A., & Ivry, R. (1989). Line segregation. *Spatial Vision*, *4*, 75–101.

Bonneh, Y., & Sagi, D. (1998). Effects of spatial configuration on contrast detection. *Vision Research*, *38*, 3541–3553.

Fechner, G. T. (1858). Uber ein Psychphysisches Grundgesetz. *Abh. Lpz Ges., V1*, 457–532.

Field, D. J., Hayes, A., & Hess, R. F. (1993). Contour integration by the human visual system: evidence for a local 'association field'. *Vision Research*, *33*, 173–193.

Gallant, J. L., Braun, J., & Van Essen, D. C. (1993). Selectivity for polar, hyperbolic, and Cartesian gratings in macaque visual cortex. *Science*, *259*, 100–103.

Gilbert, C. D., Das, A., Ito, M., Kapadia, M., & Westheimer, G. (1996). Spatial integration and cortical dynamics. *Proceedings of the National Academy of Sciences of the USA*, *93*, 615–622.

Hess, R. R, Dakin, S. C., & Field, D. J. (1998). The role of 'contrast enhancement' in the detection and appearance of visual contours. *Vision Research*, *38*, 783–787.

Hu, Q., Klein, S. A., & Carney, T. (1993). Can sinusoidal vernier acuity be predicted by contrast discrimination? *Vision Research*, *33*, 1241–1258.

Kapadia, M. K., Ito, M., Gilbert, C. D., & Westheimer, G. (1995). Improvement in visual sensitivity by changes in local context: parallel studies in human observers and in V1 of alert monkeys. *Neuron*, *15*, 843–856.

Keeble, D. R., & Hess, R. F. (1998). Orientation masks 3-gabor alignment performance. *Vision Research*, *38*, 827–840.

Keeble, D. R. T., & Hess, R. F. (1999). Discriminating local continuity in curved figures. *Vision Research*, *39*, 3287–3299.

Klein, S. A., & Levi, D. M. (1987). The position sense of the peripheral retina. *Journal of the Optical Society of America*, *A*, *4*, 1543–1553.

Kooi, F. L., De Valois, R. L., & Switkes, E. (1991). Spatial localization across channels. *Vision Research*, *31*, 1627–1631.

Kovacs, L., & Julesz, B. (1993). A closed curve is much more than an incomplete one: effect of closure in figure-ground segmentation. *Proceedings of the National Academy of Sciences of the USA*, *90*, 7495–7497.

Lamme, V., & Spekreijse, H. (1998). Neuronal synchrony does not represent texture segregation. *Nature*, *396*, 362–366.

Levi, D. M., & Klein, S. A. (1987). Position sense of the peripheral retina. *Journal of the Optical Society of America*, *A*, *4*, 1543–1553.

Levi, D. M., & Klein, S. A. (1989). Both separation and eccentricity can limit precise position judgements: a reply to Morgan and Watt. *Vision Research*, *29*, 1463–1469.

Levi, D. M., & Klein, S. A. (1990). The role of separation and eccentricity in encoding position. *Vision Research*, *30*, 557–585.

Levi, D. M., & Klein, S. A. (1986). Sampling in spatial vision. *Nature*, *320*, 360–362.

Levi, D. M., & Klein, S. A. (2000). Detecting disorder in spatial vision. *Vision Research*, *40*, 2307–2327.

Levi, D. M., Jiang, B., & Klein, S. A. (1990). Spatial interval discrimination with blurred lines: black and white are separate but not equal at multiple spatial scales. *Vision Research*, *30*, 1735–1750.

Levi, D. M., & Sharma, V. (1998). Integration of local orientation in strabismic amblyopia. *Vision Research*, *38*, 775–781.

Levi, D. M., & Waugh, S. J. (1996). Position acuity with opposite-contrast polarity features: evidence for a nonlinear collector mechanism for position acuity? *Vision Research*, *36*, 573–588.

Levi, D. M., & Westheimer, G. (1987). Spatial-interval discrimination in the human fovea: what delimits the interval? *Journal of the Optical Society of America*, *A*, *4*, 1304–1313.

Morgan, M. J. M., & Watt, R. J. (1989). The Weber relationship for position is not an artefact of eccentricity. *Vision Research*, *29*, 1457–1463.

Nothdurft, H. (1987). Sensitivity for structure gradient in texture discrimination tasks. *Vision Research*, *25*, 1957–1968.

O'Shea, R. P., & Mitchell, D. E. (1990). Vernier acuity with opposite-contrast stimuli. *Perception*, *19*, 207–2211.

Parent, P., & Zucker, S. (1989). *IEEE Transactions on Pattern Analysis and Machine Intelligence*, *11*, 823–839.

Pettet, M. W., McKee, S. P., & Grzywacz, N. M. (1998). Constraints on long range interactions mediating contour detection. *Vision Research*, *38*, 865–879.

Polat, U., Mizobe, K., Pettet, M. W., Kasamatsu, T., & Norcia, A. M. (1998). Collinear stimuli regulate visual responses depending on cell's contrast threshold. *Nature*, *391*, 580–584.

Polat, U., & Sagi, D. (1993). Lateral interactions between spatial channels: suppression and facilitation revealed by lateral masking experiments. *Vision Research*, *33*, 993–999.

Regan, D., & Hamstra, S. J. (1992). Shape discrimination and the judgement of perfect symmetry. *Vision Research*, *32*, 1845–1864.

Saarinen, J., & Levi, D. M. (1999). The effect of contour closure on shape perception. *Spatial Vision*, *12*, 227–238.

Saarinen, J., & Levi, D. M. (2000) Integration of local features into a global pattern in human vision. (submitted).

Saarinen, L, Levi, D. M., & Shen, B. (1997). Integration of local pattern elements into a global shape in human vision. *Proceedings of the National Academy of Sciences of the USA*, *94*, 8267–8271.

Schwartz, E. L., Desimone, R-, Albright, T., & Gross, C. G. (1983). Shape recognition and inferior temporal neurons. *Proceedings of the National Academy of Sciences of the USA*, *80*, 5776–5778.

Sullivan, G. D., Oatley, K., & Sutherland, N. S. (1972). Vernier acuity as affected by target length and separation. *Perception and Psychophysics*, *12*, 438–444.

Toet, A., & Koenderink, J. J. (1988). Differential spatial displacement discrimination thresholds for Gabor patches. *Vision Research*, *28*, 133–143.

Whitaker, D., & McGraw, P. V. (1998). Geometric representation of the mechanisms underlying human curvature detection. *Vision Research*, *38*, 3843–3848.

Whitaker, D., & Latham, K. (1997). Disentangling the role of spatial scale, separation and eccentricity in Weber's law for position. *Vision Research*, *37*, 515–524.

Wilkinson, R., Wilson, H., & Habak, C. (1998). Detection and recognition of radial frequency patterns. *Vision Research*, *38*, 3555–3568.

Zanker, J. M., & Quenzer, T. (1999). How to tell circles from ellipses: perceiving the regularity of simple shapes. *Fiaturwissenschaften*, *86*, 492–495.